Mechanistic Studies of Pd(II)-Catalyzed *E/Z* Isomerization of Unactivated Alkenes: Evidence for a Monometallic Nucleopalladation Pathway

Rei Matsuura, Malkanthi K. Karunananda, Mingyu Liu, Nhi Nguyen, Donna G. Blackmond, and Keary M. Engle*

Department of Chemistry, The Scripps Research Institute, La Jolla, CA 92037 USA

ABSTRACT: Pd(II)-catalyzed *E/Z* isomerization of alkenes is a common process—yet its mechanism remains largely uncharacterized, particularly with non-conjugated alkenes. In this work, the mechanism of Pd(II)-catalyzed *E/Z* isomerization of unactivated olefins containing an aminoquinoline-based amide directing group is probed using *in situ* kinetic analysis, spectroscopic studies, kinetic modeling, and DFT calculations. The directing group allows for stabilization and monitoring of previously undetectable intermediates. Collectively, the data are consistent with isomerization occurring through a monometallic nucleopalladation mechanism.

INTRODUCTION

The activation of alkenes by Pd(II) species is a foundational reactivity paradigm in homogeneous catalysis. While palladium(II)–olefin complexes most commonly undergo nucleopalladation with suitable nucleophiles via π-Lewis acid activation,[1] several other mechanistic possibilities exist, including π-allyl formation, C(alkenyl)–H activation, alkene migration, and *E/Z* isomerization (Scheme 1).[2-4] It is critical to understand: (1) the factors that dictate which pathway is predominantly operative under a given set of reaction conditions, (2) how these processes are interconnected, and (3) the mechanistic details of each of the different pathways.

The isomerization of alkenes with a variety of Pd(II) precatalysts has been appreciated as a ubiquitous process since as early as 1964.[2,5] Positional isomerization (alkene migration), *E/Z* isomerization, or a combination of these two processes take place with a variety of substituted alkene substrates, and these processes have garnered interest both from a synthetic[6] and mechanistic[7,8] perspective over the ensuing decades. Alkene isomerization processes are attractive in preparative synthetic chemistry, as they are 100% atom-economical. Widely accessible alkene feedstocks can thus be converted into value-added isomeric products or into further functionalized target compounds through integration into tandem catalytic processes.[9-11] Harnessing the full synthetic potential of these processes, however, hinges on a refined mechanistic understanding, such that they can be controlled and rationally optimized.

Scheme 1: Olefin activation by Pd(II).

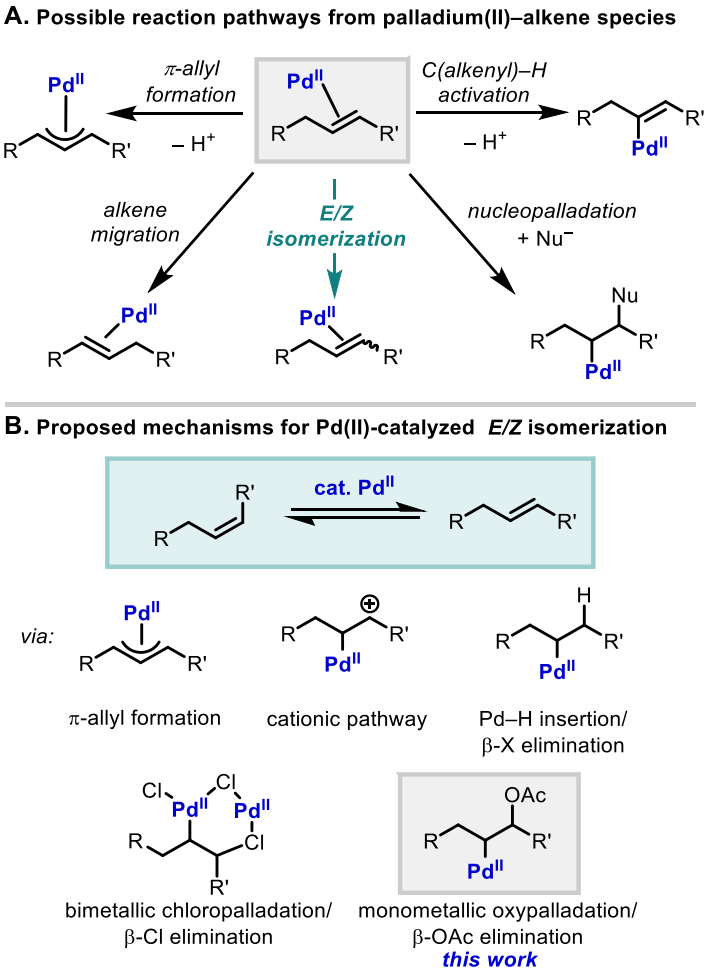

During the course of research into 8-aminoquinoline (AQ)-directed Pd(II)-catalyzed functionalization of unactivated alkenes, we observed *E/Z* isomerization of internal alkenes under various reaction conditions with $Pd(OAc)_2$ as the catalyst.[12] This reactivity was then exploited in two stereoconvergent systems.[10,11] No alkene migration was observed despite the use of unactivated alkenes in these reactions, making this an ideal model system for elucidating the mechanistic details of *E/Z* isomerization. Furthermore, the AQ directing group can stabilize catalytically competent organopalladium complexes, allowing for characterization and *in situ* monitoring of previously undetectable intermediates by NMR spectroscopy.[11] To our knowledge, a detailed study of Pd(II)-catalyzed alkene *E/Z* isomerization of electronically neutral alkenes, without complication by alkene migration, has not been carried out. Moreover, there is a lack of in-depth studies on isomerization reactions that employ Pd(II) precatalysts bearing carboxylate ligands, which are among the most widely used palladium species in organic synthesis.[13] We were interested in utilizing the system shown in Scheme 3 to study this common, yet surprisingly uncharacterized process. Deuterium-labeling experiments and *in situ* kinetic analysis under various conditions are consistent with a nucleopalladation mechanism, which is further supported by DFT calculations. Kinetic modeling of time course profiles allows for determination of relative rate constants of each step.

BACKGROUND

One of the first mechanistic investigations of Pd(II)-catalyzed *E/Z* isomerization was reported in 1972 by Henry, where the authors examined enol ethers, a type of activated alkene, as substrates (Scheme 2A).[8a] Henry's mechanistic studies allowed him to rule out the then-prevailing mechanistic hypotheses for alkene migration:[2] inter-molecular hydride transfer *via* a palladium–hydride (or π-allyl-palladium–hydride), and reversible formation of a π-allyl-palladium complex. The two possible π-allyl pathways were ruled out based on the fact that isomerization still took place with substrates lacking *β*-hydrogens. The hydride mechanism was ruled out due to lack of deuterium exchange upon using deuterated solvents.

In 1981 Sen and Lai reported the use of biscationic $Pd(MeCN)_4(BF4)_2$ as an active isomerization catalyst, with significantly different reactivity compared to neutral Pd(II) precatalysts, such as $Pd(OAc)_2$. This Pd species was found to catalyze the conversion of *tert*-butylethylene to tetramethylethylene, consistent with the intermediacy of a carbocation (Scheme 2B).[14] In a separate study of the synthesis of (*E*)-arylalkenes from (*Z*)-arylalkenes, Spencer and colleagues noted that substrates containing electron-withdrawing groups required longer reaction times, which the authors noted was potentially consistent with a cationic or chloropalladation pathway (Scheme 2C).[6b] Most recently in 2011, Lloyd-Jones, Harvey, and coworkers studied the *E/Z* isomerization of *β*-methylstyrene (Scheme 2D).[8b] Experimental studies suggested that the lowest energy pathway did not involve a carbocation intermediate, which was then reinforced by DFT calculations, ultimately supporting a binuclear non-ionic chloropalladation pathway.

Many mechanistic studies of *E/Z* isomerization have focused on styrenes or related alkenes that lack *β*-hydrogens, thereby circumventing the issue of alkene migration. The *E/Z* isomerization of non-conjugated alkenes has been less thoroughly studied, and it is unclear to what extent the mechanistic insights obtained from studies of styrenes and other conjugated alkenes are generalizable to these systems. This knowledge gap motivated the present study.

Scheme 2: Examples of alkene *E/Z* isomerization under non-hydrogenative conditions.

A. Enol propionates [Henry, 1972]

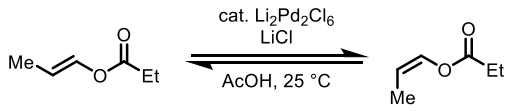

B. Tertiary carbocation probe [Sen and Lai, 1981]

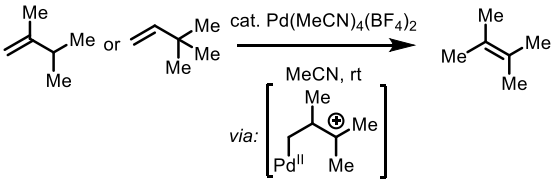

C. (*Z*)-1-phenylpropene derivatives [Spencer and coworkers, 2002]

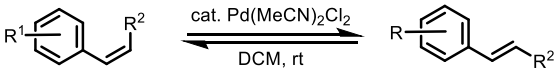

- *electron-deficient C(benzyl) in transition state*

D. (*Z*)-1-phenyl-2-butene / (*Z*)-1-phenylpropene [Lloyd-Jones, Harvey, and coworkers, 2011]

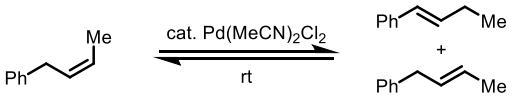

- *π-allyl ruled out by deuterium incorporation experiments*
- *reaction complicated by alkene migration* ■ *carbocation intermediate unlikely*

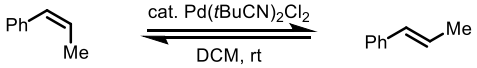

- *>1st-order in [Pd]* ■ *bimetallic chloropalladation supported by DFT*

RESULTS AND DISCUSSION

Scheme 3 shows the standard reaction conditions identified based on past work.[10,15] Control experiments verified that *E/Z* isomerization does not occur without the palladium catalyst. Without acetic acid, isomerization is observed at a diminished rate (see SI). Other internal alkene substrates also underwent *E/Z* isomerization under these conditions, indicating that this transformation is not unique to substrate **1** (see SI). Reaction progress monitoring showed an immediate drop in mass balance (**1-*Z*** + **1-*E***) at the onset of the reaction corresponding roughly to the catalyst concentration. It is proposed that this is due to formation of stable palladium(II)–alkene complexes.

Scheme 3: Pd-catalyzed E/Z isomerization.

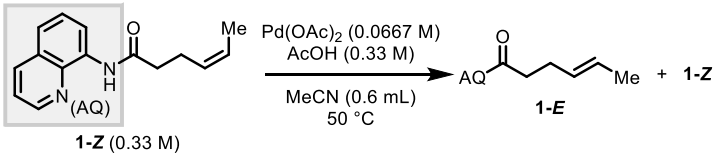

Mixtures of **1-*E*** and palladium acetate studied by ^{1}H-NMR spectroscopy allowed us to identify two Pd intermediate species (Figure 1). NOESY spectra showed that the alkenes in both complexes were in the *E*-conformation (Figure 2),[11] which we refer to as **1-Pd*E*** (major species) and **1-Pd*E'*** (minor species).

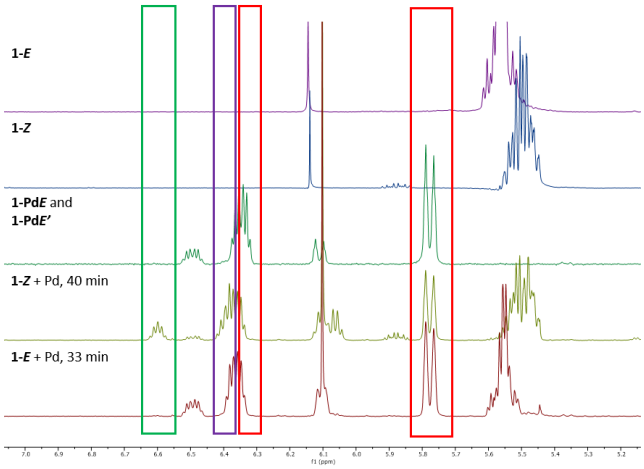

Figure 1: Comparison of various ^{1}H-NMR spectra, from top to bottom: alkene **1-*E***; alkene **1-*Z***; isolated **1-Pd*E*** and **1-Pd*E'***; 40 min after adding $Pd(OAc)_2$ to **1-*Z***; 33 min after adding $Pd(OAc)_2$ to **1-*E***. All spectra were taken at room temperature.

Comparison of these spectra showed that the intermediates **1-Pd*E*** and **1-Pd*E'*** persisted throughout the reaction (Figure 1, red box), and two additional palladium–alkene complexes were observed. These two new complexes (Figure 1, green and purple boxes) were observed at earlier time points when starting the reaction with **1-*Z***. At later time points, the size of these peaks decreased, while those of **1-Pd*E*** increased. Based on the shape and splitting of the peaks of these two unknown complexes, we propose that these peaks are the *Z*-configured analogues of **1-Pd*E*** and **1-Pd*E'***, which hereafter we refer to as **1-Pd*Z*** and **1-Pd*Z'***(see SI for detailed analysis). Attempts to isolate the complexes formed via treatment of **1-*Z*** with palladium acetate for more detailed NMR characterization were unsuccessful.

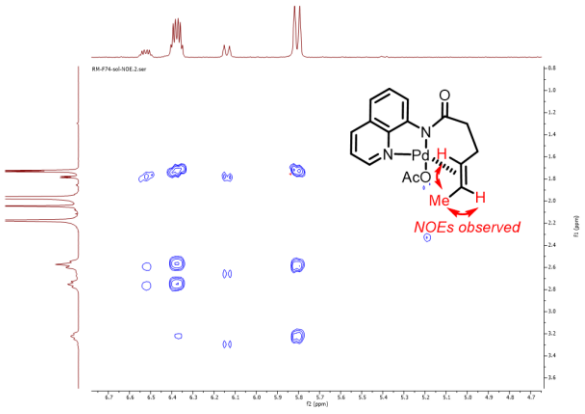

Figure 2. NOESY spectrum of **1-Pd*E*** and **1-Pd*E'***, showing the through-space interactions of the alkenyl protons and the methyl protons.

In situ NMR spectroscopy allowed us to monitor intermediates **1-Pd*Z*** and **1-Pd*E***, as well as **1-*Z*** and **1-*E***, over the course of the reaction. Starting from **1-*Z***, the observed reaction progress is characterized by an immediate drop in [**1-*Z***] that is roughly equivalent to the concentration of Pd, concomitant with formation of **1-Pd*Z***, followed by a decrease of **1-Pd*Z*** and increase in **1-Pd*E*,** implying that **1-*Z*** binds rapidly and strongly to the palladium catalyst to form **1-Pd*Z***, which then undergoes *E/Z* isomerization to form **1-Pd*E***. Finally, dissociation releases **1-*E*** and regenerates the palladium catalyst. The entire reaction sequence is reversible and equilibrates over time to give the equilibrium distribution [**1-*E***]/[**1-*Z***] ratio of K_{eq} = ca. 3.7. From the NMR spectra, we were able to experimentally determine the ratio [**1-Pd*E***]/[**1-Pd*Z***] at equilibrium as K_{iso} = ca. 7. These steps are shown in Scheme 4, where 'Pd' stands for $Pd(OAc)_2$.

Scheme 4: Proposed elementary steps in the isomerization reaction.

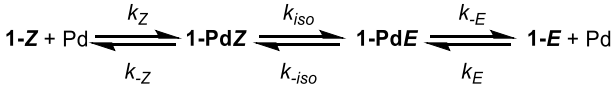

Kinetic profiles were obtained in reactions with different starting ratios of *Z*:*E* using ^{1}H-NMR to monitor the reaction. COPASI modeling[16] was then used to fit the data to estimate the rate constants. Considering both forward and backward steps, there are 6 total rate constants to consider. If we define the following equilibrium constants (eq 1):

$$K_E = \frac{k_E}{k_{-E}}, K_Z = \frac{k_Z}{k_{-Z}}, K_{iso} = \frac{k_{iso}}{k_{-iso}}, K_{eq} = \frac{[E]_{eq}}{[Z]_{eq}} \quad (1)$$

then K_{eq} becomes (eq 2):

$$K_{eq} = \frac{K_Z * K_{iso}}{K_E} = \frac{k_Z * k_{iso} * k_{-E}}{k_{-Z} * k_{-iso} * k_E} \quad (2)$$

and therefore k_{iso} becomes (eq 3):

$$k_{iso} = \frac{K_{eq} * k_{-Z} * k_{-iso} * k_E}{k_Z * k_{-E}} \quad (3)$$

Therefore, the rate constants may be defined in the following manner:

$$k_Z = k_{-Z} * K_E * \frac{K_{eq}}{K_{iso}} \quad (4)$$

$$k_E = k_{-E} * K_E \quad (5)$$

$$k_{iso} = K_{iso} * k_{-iso} \quad (6)$$

We give K_{eq} and K_{iso} their experimentally measured values and treat k_{-Z}, k_{-E}, k_{-iso} and K_E as variables. Setting the parameter k_{-iso} arbitrarily at a range of values did not alter the values of the other variables, and therefore we set k_{-iso} as 1 min^{-1} (see SI for details). The simultaneous fit to multiple data sets under different reactant concentrations gave an excellent fit, as shown in Figure 3. Parameter estimation of these four variables gave the following results as listed in Table 1, within 5% variation (see SI for details).

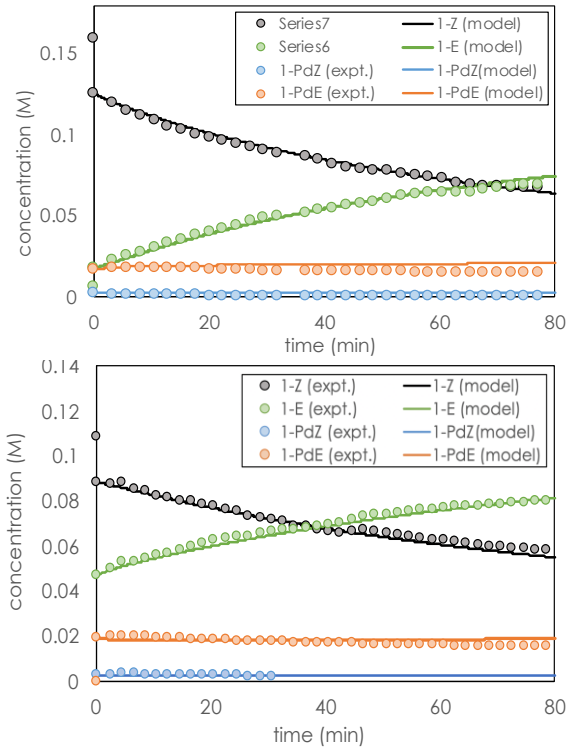

Figure 3. COPASI fit compared to the kinetic profile of the isomerization reaction of Scheme 4 in CD_3CN at 50 °C. Top: **1-*Z*** (0.159 M); **1-*E*** (0.006 M); $Pd(OAc)_2$ (0.034 M); AcOH (0.186 M). Bottom: **1-*Z*** (0.109 M); **1-*E*** (0.0531 M); $Pd(OAc)_2$ (0.032 M); AcOH (0.186 M).

This kinetic modeling reveals that the concentration of **1-Pd*Z*** remains ca. an order of magnitude lower than that of **1-Pd*E*** throughout the reaction. Although the equilibrium constants of the two Pd complexes differ only by a factor of 2, their equilibrium concentrations are influenced by the [**1-*E***]/[**1-*Z***] equilibrium ratio, as shown in eq (7).

Table 1: Results of COPASI fitting using NMR data sets and definition listed above.

Rate constants		Equilibrium constants	
k_Z	1.43 ($M^{-1}\cdot min^{-1}$)	K_Z	17.2 (M^{-1})
k_{-Z}	0.0830 ± 0.0026 (min^{-1})	K_E	32.6 ± 1.09 (M^{-1})
k_{iso}	7 (min^{-1})	K_{iso}	7
k_{-iso}	1 (min^{-1}, defined)	K_{eq}	3.7
k_E	3.28($M^{-1}\cdot min^{-1}$)		
k_{-E}	0.101 ± 0.005 (min^{-1})		

$$\frac{[\mathbf{1\text{-}PdE}]_{eq}}{[\mathbf{1\text{-}PdZ}]_{eq}} = \frac{K_E}{K_Z} \cdot \frac{[\mathbf{1\text{-}E}]_{eq}}{[\mathbf{1\text{-}Z}]_{eq}} \cong 7 \quad (7)$$

Having established the kinetic behavior of this catalytic isomerization, we next explored the mechanism through which the isomerization occurs. Based on the literature, there are three main candidate mechanisms for alkene *E/Z* isomerization under the palladium(II)-catalyzed conditions in this system: (1) via π-allylpalladium(II) formation, (2) via nucleometallation/*β*-elimination, and (3) via π-Lewis acid activation to form a carbocation.[2-5,8] Given that we have previously shown that alkene **1-*Z*** is capable of undergoing C(alkenyl)–H activation in the presence of palladium(II),[10] we also considered a fourth mechanism for *E/Z* isomerization involving: (4) C(alkenyl)–H activation to form an alkenylpalladium(II) species, followed by isomerization via a η^2-alkenyl-palladium/metallocarbene intermediate, in analogy to previous proposals to rationalize *E/Z* isomerization in the Pd(0)-catalyzed cross-coupling of alkenyl reaction partners.[13c,17]

First, deuterium-labeling studies allowed us to rule out formation of a π-allylpalladium species, as in (1), as no migration or loss of deuterium labels at either of the allylic positions was observed (Scheme 5A, B). Next,[17] to test the viability of pathway (4), we prepared alkenyl-D-labeled substrate **1-*Z*-d$_2$**. When it was subjected to the standard isomerization conditions, H/D exchange at the γ-carbon was indeed observed, consistent with our previous report (Scheme 5C).[10] Examination of the rate profile revealed that at low conversion, the *E*-alkene that is formed is primarily D_2-labeled and that rate of isomerization is much higher than the rate of H/D exchange, which is inconsistent with this pathway (see SI for details). Indeed, DFT calculations indicated that the barrier for C(alkenyl)–H activation is higher than the activation energy for every step in pathway (2) (see SI).

Scheme 5: Deuterium-labeling studies.

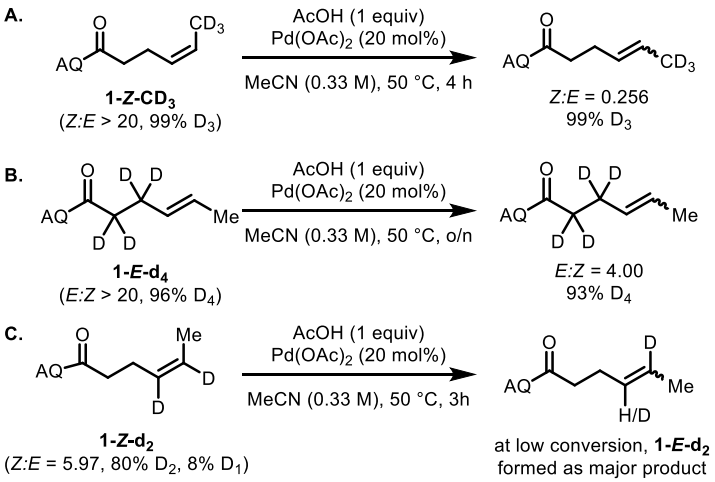

Unfortunately, deuterium-labeling studies do not allow for differentiation between (2) the nucleometallation/β-elimination pathway and (3) the cationic pathway. Under our reaction conditions, acetate would be the most likely nucleophile in a nucleometallation/*β*-elimination pathway. Therefore, we reasoned that if AcOH were removed from the system, this should suppress the reaction rate if a nucleometallation/*β*-elimination were operative. To test this, we performed the reaction with $Pd(MeCN)_4(BF_4)_2$ instead of $Pd(OAc)_2$, Indeed, the reaction rate was heavily reduced (see SI). This further suggests that the cationic pathway is unlikely, as Sen and Lai had previously observed this catalyst gave enhanced reactivity in alkene isomerization (via a presumed cationic pathway). Adding AcOH to the reaction with $Pd(MeCN)_4(BF_4)_2$ as the catalyst does not give an increase in rate. The origin of this observation is unclear but could potentially be due to inefficient ligand exchange of acetate under these conditions. To further probe the viability of the cationic pathway, we subjected *Z*-configured, *tert*-butyl-containing alkene **2** to the reaction conditions and found that the alkene underwent *E/Z* isomerization without migration of the methyl group (Scheme 6). This suggests that a tertiary cation was not formed,[14] which is inconsistent with a cationic pathway.

Scheme 6: Pd-catalyzed *E/Z* isomerization.

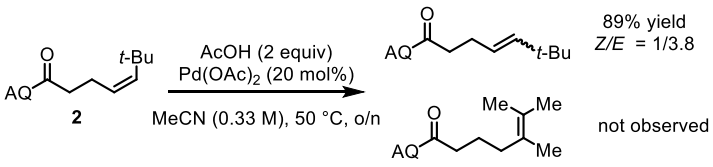

DFT calculations were used to further examine the likelihood of a monometallic nucleopalladation pathway (Figures 5, 6). First, the two experimentally observed conformers of the π-coordinated alkene complex, **1-Pd*E*** and **1-Pd*E'*** were located. Subsequent calculations focused on the lower-energy conformer, **1-Pd*E***, as the transition state for the *anti*-nucleopalladation from the higher-energy conformer, **1-Pd*E'***, was found higher, and other steps were expected to follow the same trend (see SI). Next, the regioselectivity of the alkene addition event was examined. Transition states for nucleophilic attack on the γ-carbon (Figure 5, blue) and the δ-carbon (Figure 5, black) were computed, favoring attack of the δ-carbon by 6.5 kcal/mol. This is consistent with our previous observations that the palladium catalyst is more likely to form a 6-membered palladacycle than a 7- membered palladacycle on both kinetic and thermodynamic grounds.[18]

Next, the optimized transition state for the nucleophilic attack was compared to that of the solvent-coordinated carbocation formed via π-Lewis acid activation (Figure 5, red). Consistent with our above hypothesis, the carbocation was higher in energy by 4.5 kcal/mol. The activation barrier for the carbocation formation is expected to be much higher in energy rendering the cationic pathway highly unfavorable. Attempts to locate a transition state have been unfruitful.[8b]

Figure 5. Computed carbocation intermediate (red), and transition states for the nucleophilic attack on the γ-carbon (blue) and δ-carbon (black).

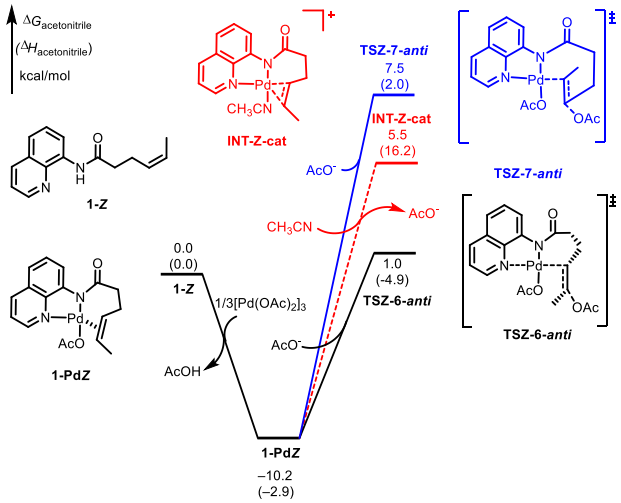

Finally, the overall reaction profile was calculated as shown in Figure 6.[19] Both the *syn*- and *anti*-nucleopalladation pathways (and thus the microscopic reverses) were sufficiently low in energy to make the monometallic nucleopalladation pathway viable, even under mild conditions. The lowest energy pathway (Figure 6, black) begins with the π-alkene–palladium complex of the *Z*-alkene (**1-Pd*Z***) undergoing *anti*-nucleopalladation. Acetate is intimately involved as the nucleophile in this process, consistent with the requirement of a carboxylic acid additive and the absence of reactivity observed with cationic catalysts. The *syn*-pathway is higher in energy than the *anti*-pathway, consistent with previous observations for AQ-directed intermolecular nucleopalladation with carbon, nitrogen, and oxygen nucleophiles.[20] In geometrically constrained systems, both *syn*- and *anti*-β-N-eliminations have been documented, supporting the notion that while the *anti*-pathway is lower in energy, both pathways are energetically accessible, Next, bond rotation followed by β-OAc elimination gives the π-alkene–palladium complex of the *E*-alkene (**1-Pd*E***) which dissociates to release **1-*E***. All energies were significantly lower compared to β-hydride eliminations computed for similar substrates (18.0 kcal/mol)[18] which explains the lack of Wacker or chain-

walking products in the product distribution. The calculations confirm the trend of the relative stability of **1-Pd*Z*** and **1-Pd*E*** experimentally observed by NMR and predicted via kinetic modeling.

This proposed mechanism differs from that reported by Lloyd-Jones, Harvey, and coworkers for a reversible chloropalladation in the *E/Z* isomerization of β-methylstyrene catalyzed by [$(RCN)_2PdCl_2$] complexes.[8b] A number of differences between that work and ours support the proposal of different reaction mechanisms in the two cases. They observed an unusual 1.6 order dependence on Pd concentration, which they attributed to a binuclear addition/elimination mechanism. Our observation of 1st order kinetics in [Pd] under our conditions may imply that the binding of the AQ precludes the formation of the dimeric Pd complex invoked in that work. We found that the substrate employed in that work (β-methylstyrene) did not undergo isomerization under their conditions using $Pd(OAc)_2$ in place of $(RCN)_2PdCl_2$ (in DCM); additionally, substrate **1-*Z*** did not undergo isomerization neither under their conditions ($Pd(MeCN)_2Cl_2$, DCM) nor our conditions using $Pd(MeCN)_2Cl_2$ in place of $Pd(OAc)_2$ (see SI).

CONCLUSIONS

This work represents the first mechanistic investigation into metal-catalyzed *E/Z* isomerization of unconjugated alkenes that is not complicated by alkene migration. The AQ directing group enabled the stabilization of key intermediates, allowing observation and monitoring of Pd-containing complexes in addition to *Z* and *E* alkenes.

In situ kinetic analysis suggests a general mechanistic picture in which the *Z*-alkene first rapidly coordinates to the palladium catalyst while maintaining its *Z* configuration. This intermediate then undergoes *E/Z* isomerization to give a palladium–alkene complex in the *E* configuration. Finally, the palladium dissociates from the alkene to yield the *E*-alkene. Further insight into the details of the elementary steps that comprise the isomerization process is provided by deuterium-labeling experiments and DFT calculations, which support an *anti*-nucleopalladation/*β*-elimination pathway.

This work serves to advance our ultimate goal of achieving a comprehensive mechanistic understanding of the activation of alkenes by Pd(II) species and the pathways that can ensue. In particular, we have teased out the intimate connection between the nucleopalladation and *E/Z* isomerization pathways and shed light on the role of an oxygen nucleophile in isomerization. This refined understanding sets the stage for rational optimization of *E/Z* isomerization processes for synthetic applications.

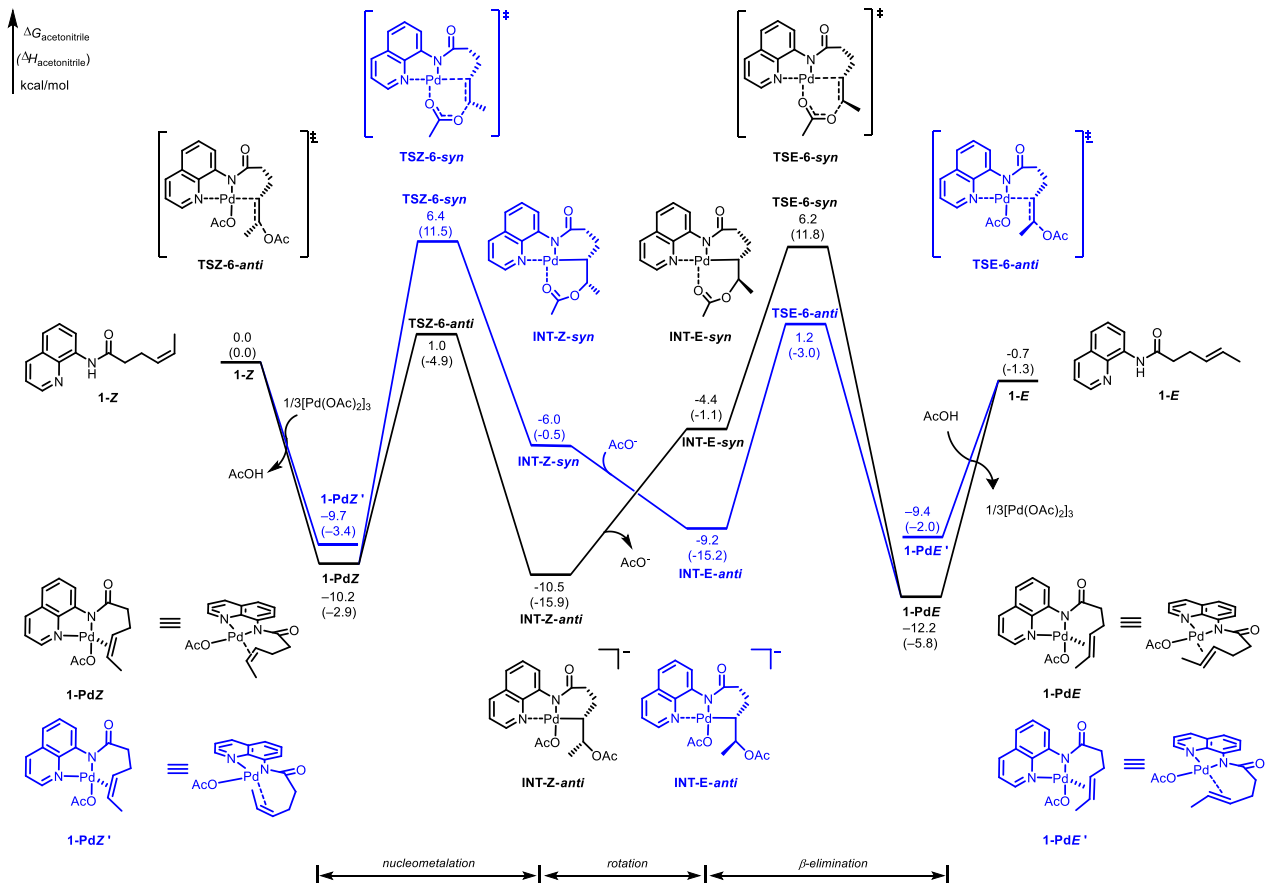

Figure 6: Computed energy profile for the *E/Z* isomerization reaction of **1-*Z*** to **1-*E***.

Supporting Information. Experimental details and details of stochastic modeling. This material is available free of charge via the Internet at http://pubs.acs.org.

AUTHOR INFORMATION

Corresponding Author

* keary@scripps.edu

ORCID

0000-0002-3334-6492 (R.M.)
0000-0002-8697-8864 (M.K.K.)
0000-0003-4649-7393 (M.L.)
0000-0001-9829-8375 (D.G.B)
0000-0003-2767-6556 (K.M.E.)

ACKNOWLEDGMENT

This work was financially supported by the National Institute of Health (R35GM125052). We gratefully acknowledge additional support from the Honjo International Scholarship Foundation for a graduate fellowship (R.M.) and the Hearst Foundation for funding a summer internship (N.N.). We thank Dr. Xiaotian Qi and Prof. Peng Liu for helpful discussion.

REFERENCES

(1) For a representative review of palladium(II)-catalyzed alkene functionalization via nucleopalladation, see: McDonald, R. I.; Liu, G.; Stahl, S. S. Palladium(II)-Catalyzed Alkene Functionalization via Nucleopalladation: Stereochemical Pathways and Enantioselective Catalytic Applications. *Chem. Rev.* **2011**, *111*, 2981–3019.

(2) Hartley, F. R. Olefin and Acetylene Complexes of Platinum and Palladium. *Chem. Rev.* **1969**, *69,* 799–844.

(3) Tsuji, J. 25 Years in the Organic Chemistry of Palladium. *J. Organomet. Chem*. **1986**, *300*, 281–305.

(4) Shang, X.; Liu, Z.-Q. Transition Metal-Catalyzed C_{vinyl}–C_{vinyl} Bond Formation *via* Double C_{vinyl}–H Bond Activation. *Chem. Soc. Rev.* **2013**, *42*, 3253–3260.

(5) Davies, N. R. Palladium-Catalysed Olefine Isomerization. *Nature* **1964**, *201*, 490–491.

(6) For applications of *E/Z* isomerization in synthesis, see: (a) Giles, R. G. F.; Lee Son, V. R.; Sargent, M. V. Palladium-Assisted (*Z*)–(*E*) Isomerization of Styrenes. *Aust. J. Chem.* **1990**, *43*, 777–781. (b) Yu, J.; Gaunt, M. J.; Spencer, J. B. Convenient Preparation of *trans*-Arylalkenes via Palladium(II)-Catalyzed Isomerization of *cis*-Arylalkenes. *J. Org. Chem.* **2002,** *67*, 4627–4629. (c) Moses, J. E.; Baldwin, J. E.; Marquez, R.; Adlington, R. M.; Cowley, A. R. Studies on the Biomimetic Synthesis of SNF4435 C and D. *Org. Lett*. **2002**, *4*, 3731–3734. (d) Moses, J. E.; Baldwin, J. E.; Brückner, S.; Eade, S. J.; Adlington, R. M. Biomimetic Studies on Polyenes. *Org. Biomol. Chem.* **2003**, *1*, 3670–3684. (e) Lemaire, P.; Balme, G.; Desbordes, P.; Vors, J.-P. Efficient Syntheses of Pterulone, Pterulone B and related analogues. *Org. Biomol. Chem.* **2003**, *1*, 4209–4219. (f) Brückner, S.; Baldwin, J. E.; Adlington, R. M.; Claridge, T. D. W.; Odell, B. Thermal and Palladium Catalyzed Pericyclic Rearrangements of a Pentaene Ester. *Tetrahedron* **2004**, *60*, 2785–2788. (g) Jacobsen, M. F.; Moses, J. E.; Adlington, R. M.; Baldwin, J. E. The Total Synthesis of Spectinabilin and Its Biomimetic Conversion to SNF4435C and SNF4435D. *Org. Lett.* **2005**, *7*, 2473–2476. (h) Chandrasekhar, S.; Sultana, S. S. Stereoselective Synthesis of the C1–C20 Segment of the Microsclerodermins A and B. *Tetrahedron Lett.* **2006**, *47*, 7255–7258. (i) Seo, S.-Y.; Jung, J.-W.; Jung, J.-K.; Kim, N.-J.; Chin, Y.-W.; Kim, J.; Suh, Y.-G. Concise Synthesis of Rodgersinol and Determination of the C-10 Absolute Configuration. *J. Org. Chem.* **2007**, *72*, 666–668.

(7) For representative studies of alkene *E/Z* isomerization under hydrogenative conditions, see: (a) Yu, J.; Spencer, J. B. First Evidence That the Mechanism of Catalytic Hydrogenation with Homogeneous Palladium and Rhodium Catalysts Is Strongly Influenced by Substrate Polarity. *J. Am. Chem. Soc.* **1997**, *119*, 5257–5258. (b) Kluwer, A. M.; Koblenz, T. S.; Jonischkeit, T.; Woelk, K.; Elsevier, C. J. Kinetic and Spectroscopic Studies of the [Palladium(Ar-bian)]-Catalyzed Semi-Hydrogenation of 4-Octyne. *J. Am. Chem. Soc.* **2005**, *127*, 15470–15480. (c) Dunne, J. P.; Aiken, S.; Duckett, S. B.; Konya, D.; Almeida Leñero, K. Q.; Drent, E. Detection and Reactivity of $Pd((C_8H_{14})PCH_2CH_2P(C_8H_{14}))(CHPhCH_2Ph)(H)$ as Determined by Parahydrogen-Enhanced NMR Spectroscopy. *J. Am. Chem. Soc*. **2004**, *126*, 16708–16709.

(8) (a) Henry, P. M. Palladium (II)-Catalyzed Exchange and Isomerization Reactions. VII. Isomerization and Exchange of Enol Propionates in Acetic Acid Catalyzed by Palladium(II) Chloride. *J. Am. Chem. Soc*. **1972**, *94*, 7316–7322. (b) Tan, E. H. P.; Lloyd-Jones, G. C.; Harvey, J. N.; Lennox, A. J. J.; Mills, B. M. [$(RCN)_2PdCl_2$-Catalyzed *E/Z* Isomerization of Alkenes: A Non-Hydride Binuclear Addition-Elimination Pathway. *Angew. Chem. Int. Ed*. **2011**, *50*, 9602–9606.

(9) For reviews of regioselective alkene migration and functionalization, see: (a) Vasseur, A.; Bruffaerts, J.; Marek, I. Remote Functionalization through Alkene Isomerization**.** *Nat. Chem.* **2016,** *8*, 209–219. (b) Sommer, H.; Juliá-Hernández, F.; Martin, R.; Marek, I. Walking Metals for Remote Functionalization. *ACS Cent. Sci.* **2018**, *4*, 153–165. (c) Massad, I; Marek, I. Alkene Isomerization through Allylmetals as a Strategic Tool in Stereoselective Synthesis. *ACS Catal.,* **2020**, *10*, 5793–5804.

(10) Liu, M.; Yang, P.; Karunananda, M. K.; Wang, Y.; Liu, P.; Engle, K. M. C(alkenyl)–H Activation via Six-Membered Palladacycles: Catalytic 1,3-Diene Synthesis. *J. Am. Chem. Soc.* **2018**, *140*, 5805–5813.

(11) (a) Liu, Z.; Li, X.; Zeng, T.; Engle, K. M. Directed, Palladium(II)-Catalyzed Enantioselective *anti*-Carboboration of Alkenyl Carbonyl Compounds. *ACS Catal.* **2019**, *9*, 3260–3265. (b) Bai, Z.; Zheng, S.; Bai, Z.; Song, F.; Wang, H.; Peng, Q.; Chen, G.; He, G. Palladium-Catalyzed Amide-Directed Enantioselective Carboboration of Unactivated Alkenes Using a Chiral Monodentate Oxazoline Ligand. *ACS Catal.* **2019**, *9*, 6502–6509.

(12) Liu, Z.; Zeng, T.; Yang, K. S.; Engle, K. M. β,γ-Vicinal Dicarbofunctionalization of Alkenyl Carbonyl Compounds via Directed Nucleopalladation. *J. Am. Chem. Soc.* **2016**, *138*, 15122–15125.

(13) For examples of *E/Z* isomerization using $Pd(OAc)_2$, see: (a) Evans, M. A.; Morken, J. P. Stereoselective Synthesis of Furans by the Pd-Catalyzed Oshima-Utimoto Reaction. *Org. Lett.,* **2005**, *7*, 3367–3370. (b) Casanova, N.; Del Rio, K. P.; García-Fandiño, R.; Mascareñas, J. L.; Gulías. M. Palladium(II)-Catalyzed Annulation between *ortho*-Alkenylphenols and Allenes. Key Role of the Metal Geometry in Determining the Reaction Outcome. *ACS Catal.,* **2016**, *6*, 3349–3353. (c) Schreib, B. S.; Fadel, M.; Carreira, E. M. Palladium-Catalyzed C–H Alkynylation of Unactivated Alkenes. *Angew. Chem. Int. Ed.,* **2020**, *59,* 7818–7822.

(14) (a) Sen, A.; Lai, T. W. Catalysis by Solvated Transition-Metal Cations. Novel Catalytic Transformations of Alkenes by Tetrakis(acetonitrile)palladium Ditetrafluoroborate. Evidence for the Formation of Incipient Carbonium Ions as Intermediates. *J. Am. Chem. Soc.,* **1981**, *103*, 4627–4629. (b) Sen, A.; Lai, T. W. Catalytic Isomerization of Alkenes by Palladium(II) Compounds. An Alternative Mechanistic View. *Inorg. Chem.* **1981***, 20,* 4036–4038.

(15) The Engle Lab has previously observed that isomerization can take place in other solvents as well, and is not unique to MeCN.

(16) Hoops, S.; Sahle, S.; Gauges, R.; Lee, C.; Pahle, J.; Simus, N.; Singhal, M.; Xu, L.; Mendes, P.; Kummer, U. COPASI—a COmplex PAthway SImulator. *Bioinformatics* **2006**, *22*, 3067–3074.

(17) For representative studies of the *E/Z* isomerization of alkenylpalladium intermediates, see: (a) Chernyak, N.; Gorelsky, S.I.; Gevorgyan, V. Palladium-Catalyzed Carbocyclization of Alkynyl Ketones Proceeding through a Carbopalladation Pathway. *Angew. Chem. Int. Ed.*, **2011**, *50*, 2342–2345. (b) Aziz, J.; Frison,

G.; Le Menez, P.; Brion, J.-D.; Hamze, A.; Alami, M. Gold *versus* Palladium: A Regioselective Cycloisomerization of Aromatic Enynes, *Adv. Synth. Catal.,* **2013**, *355*, 3425–3436. (c) Pawliczek, M.; Schneider, T.F.; Maaß, C.; Stalke, D.; Werz, D.B. Formal *anti*-Carbopalladation Reactions of Non-Activated Alkynes: Requirements, Mechanistic Insights, and Applications. *Angew. Chem. Int. Ed.,* **2015,** *54*, 4119–4123. (d) Sperger, T.; Le, C. M.; Lautens, M.; Schoenebeck, F. Mechanistic Insights on the Pd-Catalyzed Addition of C–X Bonds Across Alkynes – a Combined Experimental and Computational Study. *Chem. Sci.,* **2017**, *8*, 2914–2922.

(18) O'Duill, M. L.; Matsuura, R.; Wang, Y.; Turnbull, J. L.; Gurak, J. A., Jr.; Gao, D.-W.; Lu, G.; Liu, P.; Engle, K. M. Tridentate Directing Groups Stabilize 6-Membered Palladacycles in Catalytic Alkene Hydrofunctionalization. *J. Am. Chem. Soc.* **2017**, *139*, 15576–15579.

(19) This oxypalladation/beta-elimination sequence is analogous to a proposal made by Henry for the simultaneous *E/Z* isomerization and O-exchange of vinyl ethers in the presence of Pd(II) and acetic acid. See ref. 7a and Henry, P. M. Palladium(II)-Catalyzed Exchange and Isomerization Reactions. I. Exchange of Enol Acetates with Acetic Acid Catalyzed by Palladium(II) Chloride. *J. Am. Chem. Soc.,* **1971**, *93*, 3853–3859.

(20) Tran, V. T.; Gurak, J. A., Jr.; Yang, K. S.; Engle, K. M. Activation of Diverse Carbon–Heteroatom and Carbon–Carbon Bonds via Palladium(II)-Catalyzed β-X Elimination. *Nat. Chem.,* **2018**, *10*, 1126–1133.